

Dynamic responses of an FPSO moored on sloped seabed under the action of environmental loads

Shovan Roy^a and Atul K. Banik*

Department of Civil Engineering, National Institute of Technology Durgapur, WB, India

(Received May 4, 2018, Revised August 16, 2018, Accepted August 19, 2018)

Abstract. The inclination of seabed profile (sloped seabed) is one of the known topographic features which can be observed at different seabed level in the large offshore basin. A mooring system connected between the platform and global seabed is an integral part of the floating structure which tries to keep the floating platform settled in its own position against hostile sea environment. This paper deals with an investigation of the motion responses of an FPSO platform moored on the sloped seabed under the combined action of wave, wind and current loads. A three-dimensional panel discretization method has been used to model the floating body. To introduce the connection of multi-segmented non-linear elastic catenary mooring cables with the sloped seabed, a quasi-static composite catenary model is employed. The model and analysis have been completed by using hydrodynamic diffraction code AQWA. Validation of the numerical model has been successfully carried out with an experimental work published in the latest literature. The analysis procedure in this study has been followed time domain analysis. The study involves an objective oriented investigation on platform motions, in order to identify the effects of the sloped seabed, the action of the wave, wind and current loads and the presence of riser system. In the end, an effective analysis has been performed to identify a stable mooring model in demand of reducing structural responses of the FPSO.

Keywords: sloped seabed; FPSO; wave; wind; current; quasi-static

1. Introduction

Floating Production Storage and Offloading (FPSO) forms an integral part in the emergent hydrocarbon gas and oil extracting sector. It has been globally accepted that FPSO towers over other offshore structures in terms of functionality due to its immense versatility. The ease of installation and safe operation on FPSOs ensure a settled position for the structure in the frontier of modern offshore engineering. Enormous storage capacity, lack of necessity of pipeline systems and an extended deck area are some of the salient features of this vessel, which has been a major factor for its dominance in the offshore resource market. The operating area of FPSOs being deep oceans, environmental factors are seriously considered in their design. Wave, wind, and ocean current loads are considered to be the primary environmental loads that the FPSO is subjected to. The station keeping of the platform, thus becomes a major component of the design. From the safe marine operational point of view to get precise position and motion control of this unit, is needed

*Corresponding author, E-mail: atul.banik@ce.nitdgp.ac.in

^a Ph.D. Student, E-mail: sr.14ce1504@phd.nitdgp.ac.in

to be deployed together with a slenderer single or multi-legged mooring system. These nonlinear catenary mooring cables are followed by the fairlead to partially suspended, partially grounded and then anchored at the end to the seabed. To hold the structure in the desired location a significant part of the mooring cables lies on the seabed. Besides, seabed may not be assumed as a horizontal bed.

Usan field, Offshore Nigeria is progressively exploited for hydrocarbons and consist of the variant angle of seabed slopes, water depth in between 740 and 760 m (Jones *et al.* 2013). Normally, It has a certain inclination from downstream to upstream which can never be neglected for a largely spread FPSO and it's scattered mooring system on the seabed.

A set of the simplified ship-manoeuving equation based performance and stability of turret moored FPSOs has been identified by numerous researchers namely Lee *et al.* (2000) and Sphaier *et al.* (2000). Many authors were mentioned the involvement of wind, waves, and current as external loads to the structure needs a dynamic study (Irani *et al.* 2001). The change of the motion behaviour of a turret-moored FPSO with dynamic positioning control is analysed by Kim *et al.* (2016). Among them, irregular waves with winds and currents containing a numerical study of turret moored FPSO has been comprehensively derived by Wichers (1988). He has postulated the equation of motion using the time domain uncoupled method and distinctly developed the formulation for rigid-body and cable dynamics.

In case of FPSOs, along with the mooring cables a significant number of risers are also attached to the platform (Fig. 1). As a result, the responses of the platform are also derived from the wave frequency motions of the risers, leading to mean offsets (Ormberg and Larsen 1998). This, in turn, affects the coupling interaction of the mooring and riser with the platform as well as the seabed. In existence of sloped seabed, the change in line geometry of mooring and riser affects the inline tension generation which in turn restores the platform towards the equilibrium position (Chai *et al.* 2002). Although, after surveying the numerous literature it has been found, there is scanty of literature, in which the sloped seabed effect on the structural dynamic responses with proper illustration has been addressed.

Ward *et al.* (2001) and Kim *et al.* (2005) have carried out an experiment to investigate the response of the turret-moored FPSO which was designed for 6000-ft water depth. A similar experiment has been done by Baar *et al.* (2000) to find the extreme response of a turret-moored FPSO in the Gulf of Mexico. The model tests have some limitations to calculate the interaction effects of rigid body and slender cables at deep-water condition due to depth restrictions of wave basins. Another major problem of physical model testing is differential Reynolds number between the cable lines and the prototype. Several researchers have shifted their focus to develop the modelling and simulation tools for the analysis of an FPSO. Likewise, a second order diffraction radiation panel program WAMIT has been incorporated into the hydrodynamic analysis on the turret-moored FPSO by Tahar and Kim (2003). To estimate the response behaviour of an FPSO under dynamic environment condition, the time domain analysis has been preferred more over frequency domain analysis. (Shivaji and Sen 2015).

In this paper, a new approach to modelling of an FPSO with segmented mooring system interacted with seabed has been successively adopted. Here, the large floating body has been discretized in three-dimensional panel method. Strategically, a quasi-static composite model approach has permitted the physical connection between the multi-segment elastic catenary lines with the sloped seabed. Whereas seabed interaction nodes are modelled in the sense to diminish the reactive energy losses and to minimize the discontinuity. The structural and geometrical parameters have been obtained from the work of Lopez *et al.* (2017). The validation of the model

has been carried out by comparing the natural periods from the free decay analysis and by comparing the response amplitude operators (RAOs) from the wave excitation with those obtained through experimental work by Lopez *et al.* (2017). The advantage of nonlinear modelling is also highlighted in this work which reinforces the necessity of complex nonlinear modelling in problems like the one undertaken in the current study. This paper provides an insight into a comprehensive modelling technique, where rigid floating structures can be modelled along with flexible mooring cables and the touchdown zone condition can also be incorporated.

2. Background theory

2.1 Floating body hydrodynamics

Hydrodynamic loading on a floating body is primarily caused by the kinematics of water particles in waves, resulting in motion of the structure, and finally the interaction of structure and incident waves (Faltinsen 1990). This kind of force is generally formed due to active and reactive loading components. Whereas active loading or wave exciting force is developed by the incident wave and diffraction wave and reactive loading or radiation force are generated from the radiation wave, initiated by the body motions. After identifying the wave load parameters three-dimensional potential method can be adopted in the mathematical model and the velocity potential induced by the incident $\varphi_i(x, y, z)$, diffraction $\varphi_D(x, y, z)$ and radiation waves $\varphi_R(x, y, z)$ may be summarized as follows

$$\varphi(x, y, z)e^{-i\omega t} = Re \left\{ \left[\varphi_i(x, y, z) + \varphi_D(x, y, z) + \sum_6^j \varphi_{Rj}(x, y, z)\eta_j \right] e^{-i\omega t} \right\} \begin{cases} \eta_j = u_j, (j=1,3) \\ \eta_j = \theta_{j-3}, (j=4,6) \end{cases} \quad (1)$$

Where Re is the real part of the argument. $i^2 = -1$. t and ω are the time and the wave frequency, respectively. $\varphi_{Rj}(x, y, z)$ is the radiation wave potential corresponding to the unit wave amplitude j th motion, and η_j is the wave amplitude of j th motion; u_j and θ_j are the translation and rotational motion of j th motion and $j = 1, \dots, 6$ are the body motions in 6 degree of freedom.

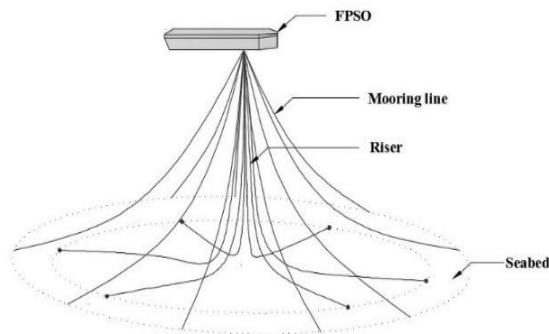


Fig. 1 FPSO platform system with riser and mooring cables

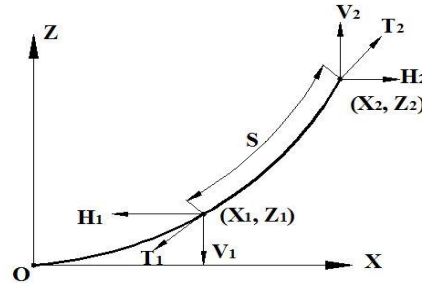


Fig. 2 Catenary line solution

Knowing the incident wave potential, a boundary element method is used to obtain the scattered wave potential. To perform a nonlinear time domain analysis, both the mean wetted hull surface and the surface above the mean water level are required to be identified. Therefore, the meshing of the structure is carried out following guidelines of the 3D panel method. The structure is discretized into a number of diffracting and non-diffracting panels. These panels must not cut the mean water surface. All the panels not involved directly in the wave force calculation are referred to as non-diffracting panels. Thereafter, the wave forces are computed by integrating the pressures on the diffracting panel surfaces. Pressure distribution on the diffracting panels is obtained from linear Bernoulli equation considering both the incident and scattered wave potentials.

2.2 Nonlinear catenary line

In the present study, a solution of the catenary equation is obtained by considering nonlinear stiffness of the line segment. A local coordinate system OXYZ is assumed, where the X axis and Y axis are lying on the surface of the seabed and positive Z axis is vertically upward, as shown in Fig. 2. The static excursions in X and Z directions of a non-linear catenary line are given as,

$$\Delta X = \frac{H}{w} \ln \frac{V_2 + T_2}{V_1 + T_1} \quad (2)$$

$$\Delta Z = \frac{T_2 - T_1}{w} \quad (3)$$

Where, ΔX and ΔZ are the horizontal and vertical extension of the catenary line segment, H is the horizontal component of tension, V_1 and V_2 are the vertical component of the tension in bottom left hand segment and top right hand segment, T_1 and T_2 are the tension force in bottom left hand segment and top right hand segment and w is the submerged weight per unit length.

The extension of the catenary line segment ΔS with equivalent nonlinear axial stiffness AE^e can be expressed as

$$\Delta S = S \frac{T^e}{AE^e} \tag{4}$$

$$AE^e = \frac{T^e}{\varepsilon} \tag{5}$$

Where T^e is denoted as equivalent tension and ε is the strain function. Here, this nonlinear stiffness values of the catenary lines are transferred to the global stiffness matrix of the equation of motion.

Here, the catenary mooring lines are divided into three segments (chain-wire-chain) and connected as an elastic member between the hull and sloped seabed. Each catenary line segments are defined by their length, mass per unit length and the equivalent cross-sectional area which is numerically equivalent to the volume of water displaced by per unit length. Also, the nonlinear axial stiffness is incorporated as a line property. The anchored point should be considered for each cable separately.

2.3 Catenary line on the sloped seabed

A catenary composite line on the global sloped seabed can be expressed by a quasi-static model, shown in Fig. 3, where the local seabed is defined as right-hand Cartesian frame OXYZ and the origin is laid on the seabed reference point. The local axes and corresponding fixed reference axes are parallel to each other. Moreover, the angle between the steepest upward path on the seabed and the horizontal plane is called seabed angle β_o and the angle between the extension of the steepest path on the horizontal plane and the local axis is defined as the azimuth angle θ_o .

The relative azimuth angle $\Delta\theta_o$ of the line in the vertical plane is

$$\Delta\theta_o = \tan^{-1} \left(\frac{z}{\vec{l} \cdot (\vec{X}_D - \vec{X}_M)} \right) \tag{6}$$

Where \vec{l} is the seabed azimuth directional vector in the fixed reference axes and the coordinate points of D and M are denoted by \vec{X}_D and \vec{X}_M respectively.

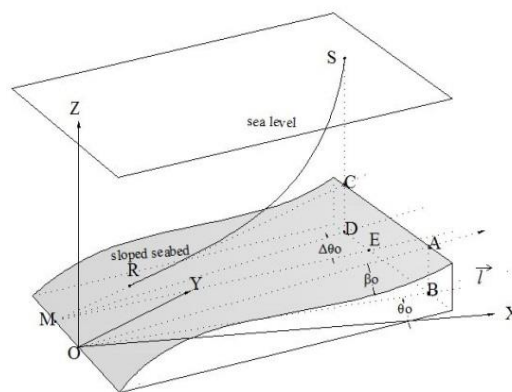


Fig. 3 Catenary line on the sloped seabed

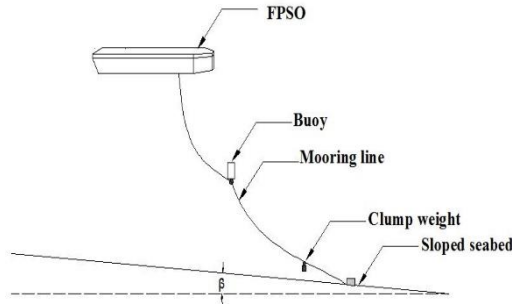


Fig. 4 Catenary composite line

In the present study, with the help of using quasi-static catenary line model, sloped seabed has been introduced with the catenary line segment. The buoys and clump weights may be attached to the catenary segment joints. A catenary composite line, anchored in a sloped seabed is shown in Fig. 4. In this quasi-static model, friction force due to a laid-down portion on the sloped seabed, current drag and inertia force of the line has not been considered.

2.4 Rigid body motion

$$\{\mathbf{M} + \mathbf{A}(\infty)\} \ddot{\mathbf{X}}(t) + \mathbf{C}\dot{\mathbf{X}}(t) + \mathbf{K}\mathbf{X}(t) + \int_0^t \mathbf{h}(t-\tau) \ddot{\mathbf{X}}(\tau) d\tau = \mathbf{F}_{hydro} + \mathbf{F}_{current} + \mathbf{F}_{wind} \quad (7)$$

Here, \mathbf{M} is the system mass matrix consisting of the structural mass component and $\mathbf{A}(\infty)$ is the added mass matrix component in infinite frequency; \mathbf{C} is the linear damping matrix, \mathbf{K} is the system stiffness matrix consisting of the contributions from the hydrostatic stiffness and mooring stiffness, \mathbf{X} is the structural displacement vector, $\dot{\mathbf{X}}$ is the structural velocity vector while $\ddot{\mathbf{X}}$ is the structural acceleration vector. \mathbf{F}_{hydro} , $\mathbf{F}_{current}$ and \mathbf{F}_{wind} represents respectively the hydrodynamic force, the current force and the wind force. Here, $\mathbf{h}(\tau)$ is the acceleration impulse function computed by the transform of the frequency-dependent added-mass matrix $\mathbf{A}(\omega)$ and hydrodynamic damping matrix $\mathbf{C}(\omega)$ in wave frequency ω

$$\mathbf{h}(\tau) = \frac{2}{\pi} \int_0^{\infty} \left[\mathbf{C}(\omega) \frac{\sin(\omega t)}{\omega} \right] d\omega = \frac{2}{\pi} \int_0^{\infty} [(\mathbf{A}(\omega) - \mathbf{A}(\infty)) \cos(\omega t)] d\omega \quad (8)$$

3. Numerical model

3.1 FPSO platform

The FPSO model used for the study was referred from the experimental work done by Lopez *et al.*

(2017). The structural properties of FPSO platform are presented in Table 1. In order to develop FPSO model, the global coordinate system has been considered for the present study, where the surface of the still water level and centreline of the platform are assumed as the origin of the axis of reference with positive z-axis vertically upwards. The three-dimensional platform model is discretized into 6051 panel elements (Fig. 5) out of which 3633 panels are diffracting elements in the draft portion. Panels in the freeboard portion are considered as non-diffracting elements.

3.2 Mooring and riser system

The mooring and riser system models are referred from the passive hybrid method based approach, carried out by Lopez *et al.* (2017). Here, the details of mooring cables and risers are taken according to the specifications provided in their truncated model at a water depth of 627 m. The particulars of mooring cable and riser are presented in Tables 2 and 3.

Table 1 The dimensions and characteristics of the FPSO

Description	Full load condition	Ballast load condition
Length LPP (m)	300	300
Breadth, B (m)	46.20	46.20
Depth, H (m)	26.20	26.20
Draught, T (m)	16.50	9.00
Ta (m)	16.50	9.50
Tf (m)	16.50	8.50
Length/Beam ratio, (L/B)	6.49	6.49
Beam/Draught ratio, (B/T)	2.80	5.13
Displacement (tonnes)	218876	122530
XB, XG (m)	2.43	3.08
ZG (m)	11.43	7.87
Kxx (m)	16.17	20.79
Kyy (m)	86.72	86.72

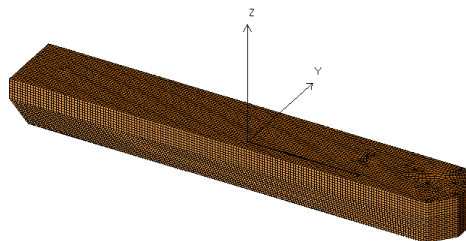


Fig. 5 FPSO panel model

Table 2 Particulars of mooring cable

Description	Prototype	Truncate specification
Number of mooring lines	9	9
Pretension (kN)	2025	2025
Total Length of mooring line (m)	2185	1160
Segment 1: Fairlead chain	R4S Studless	
Length (m)	50	50
Diameter (mm)	90	90
Mass in water (tonnes/m)	0.146	0.146
EA (kN)	691740	691740
Breaking strength (kN)	8167	-
Segment 2: Mid-section	Spiral strand	
Length (m)	1200	580
Diameter (mm)	90	90
Mass in water (tonnes/m)	0.0336	0.116
EA (kN)	766000	68000
Breaking strength (kN)	7938	-
Segment 3: Chain ground section	R4S Studless	
Length (m)	935	530
Diameter (mm)	90	90
Mass in water (tonnes/m)	0.146	0.133
EA (kN)	691740	60000
Breaking strength (kN)	8167	-

Table 3 Particulars of the riser

Description	Prototype	Truncate specification
Number of risers	6 symmetric	6 symmetric
Pretension (kN)	1500	1500
The total length of the riser (m)	2650	1400
Outside diameter (mm)	273	273
Inside diameter (mm)	235	235
Mass in water (tonnes/m)	0.096	0.234
EA (kN) Specification	3039364 API-5L-X-65	85000

4. Validation of the model

A free decay analysis of FPSO structure has been carried out in the present simulation to obtain the natural time periods and a good matched results thus comparison of natural periods are obtained as shown in Table 7.

Next, the comparisons of response amplitude operator (RAO) between the present simulation and Lopez *et al.* (2017) are depicted in Figs .6(a)-6(c) for the surge, heave and pitch response motions. The obtained numerical results compare well with the referred experimental results.

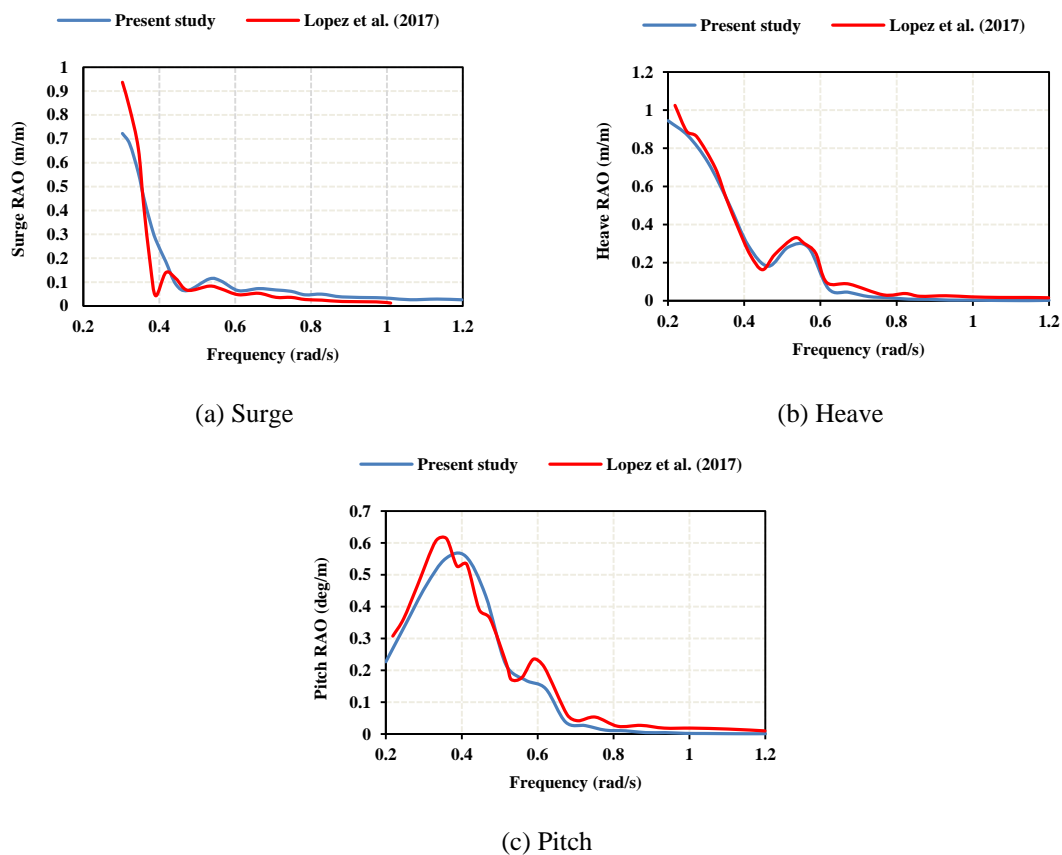


Fig. 6 RAO comparison

Table 7 Comparison of natural time periods from the present study and Lopez *et al.* (2017)

Directions	Lopez <i>et al.</i> (2017)	Present study
Surge	223.58	216.45
Sway	277.39	282.48
Heave	11.51	11.625
Roll	13.21	13
Pitch	11.60	11.16
Yaw	166.90	156.73

5. Numerical results

5.1 Comparative study

Figs. 7(a)-7(f) shows the effect of sloped bed in the structural behaviour by comparing the responses of the platform in the time domain at the sloped bed as well as a horizontal bed. To simulate the seabed profile in a more realistic manner, the slope angle is given as -4 degree as per Chai *et al.* (2002). In order to account the effects of the sloped seabed on the platform responses, wave, wind, and current have been considered and acted co-linearly from upstream to downstream direction and which is towards the positive direction of X-axis. It is clearly observed from the obtained results that significant change in motions is found due to introducing slope at the bed. In surge motion a mean offset of 32.690 m has been found because down the slope of the seabed is considered in the deeper sea that means initially the platform has shifted its location due to the cables. But there is not so much variation in response amplitude under both the seabed conditions.

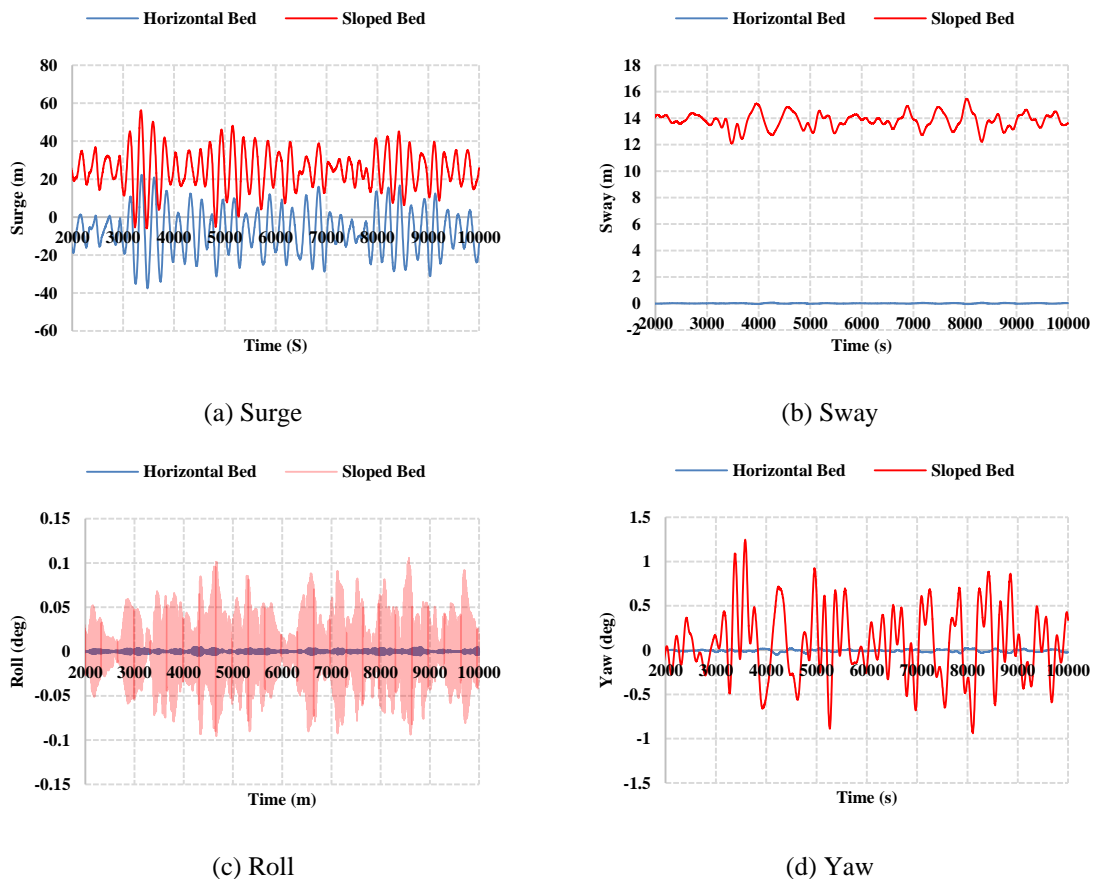


Fig. 7 Time series of a comparative study between the horizontal bed and sloped bed

However, in sway directions, the structure has shifted to 13.805 m towards positive Y direction and a significant larger amplitude response has been observed as similar to yaw and roll responses. However, the responses in heave and pitch motions are not varying so much and it should be neglected.

5.2 Effect of asymmetric stiffness

In order, to study the effect of asymmetric stiffness due to asymmetric mooring pattern between upward and downward cables which are moored on the sloped seabed as per Figs. 8(a) and 8(b), time domain analysis has been performed for group mooring and spread mooring configuration. In a randomly sloped seabed, such asymmetric mooring pattern between the cables on both the sides may produce some categorical differences in response.

Mean values and standard deviations in the surge, sway, roll and yaw responses for group mooring and spread mooring configurations are shown in Figs. 9(a)-9(d). By considering the asymmetric configuration between upward and downward moored cables the Surge, sway, roll and yaw motions are much affected. All the responses show higher fluctuation with significant standard deviation and lower responses with statistical mean values. Although due to the effect of asymmetric stiffness of mooring cables the FPSO shows larger offset in the surge and sway directions and little mean fluctuation in roll and yaw responses.

5.3 Effect of sloped seabed

The large floating structure like FPSO has required a stronghold in deep water to the bottom seabed with flexible mooring cables. Besides for seabed of the ocean domain like Usan offshore field has a number of multi-slopes which are having a certain inclination from downstream to the upstream sea floor and those cannot be ignored in response calculation. To study the seabed inclination effects on platform response, a significant time domain analysis has been carried out. All the mooring properties which are used for the flat seabed kept same in the sloped seabed. The angle between the sloping-floor to the flat seabed defined as β or angle of seabed inclination, as shown in Fig.10 and β are given as 2, 4, 6 and 8.

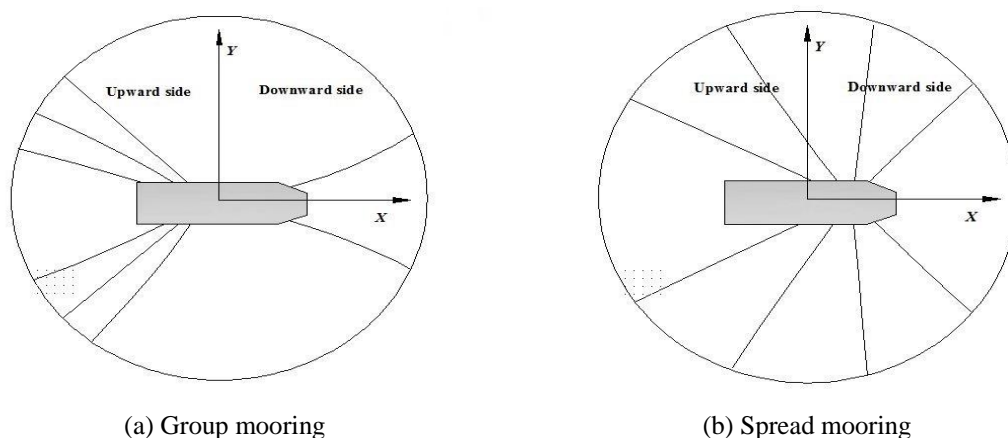


Fig. 8 Asymmetric mooring configuration

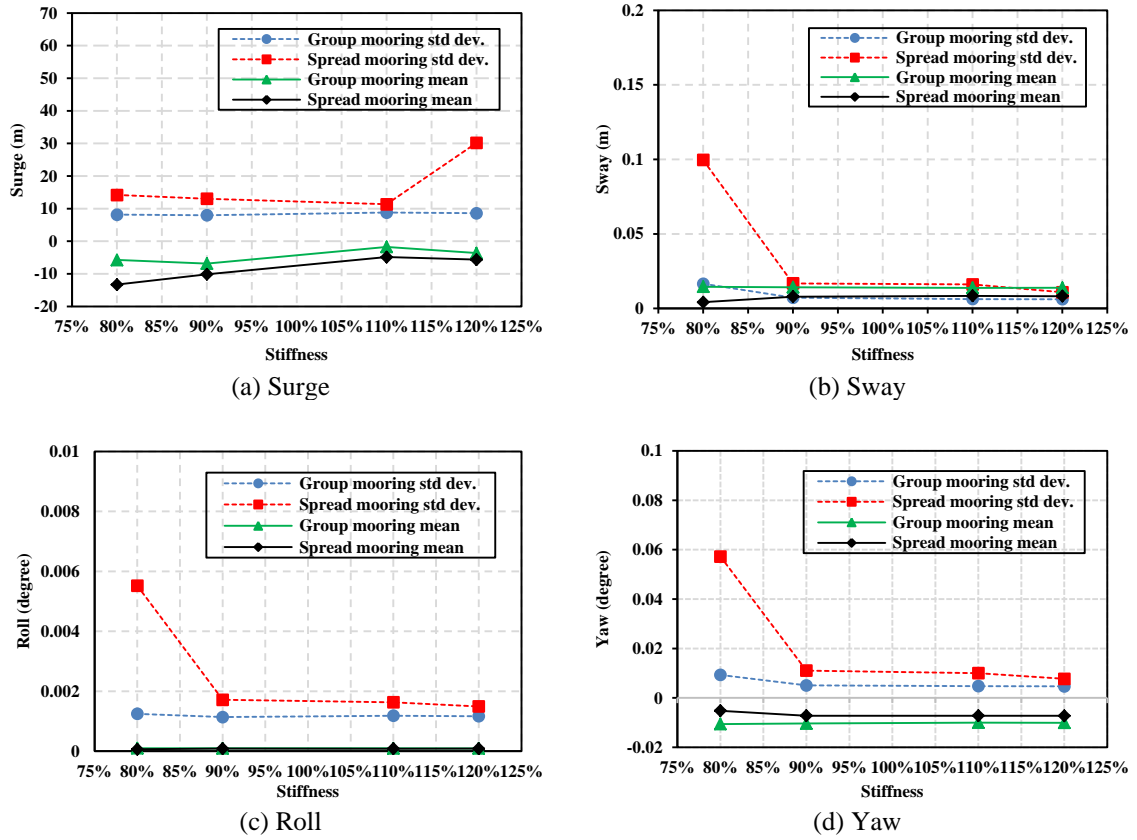


Fig. 9 Effect of asymmetric stiffness

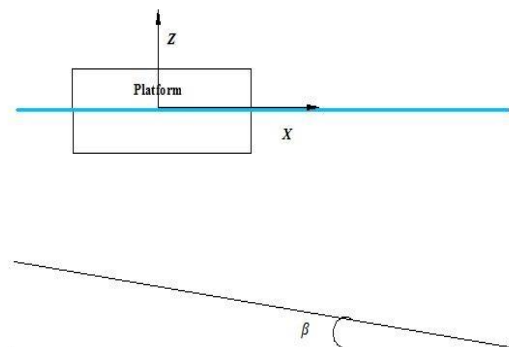


Fig. 10 The topography of the sloped seabed

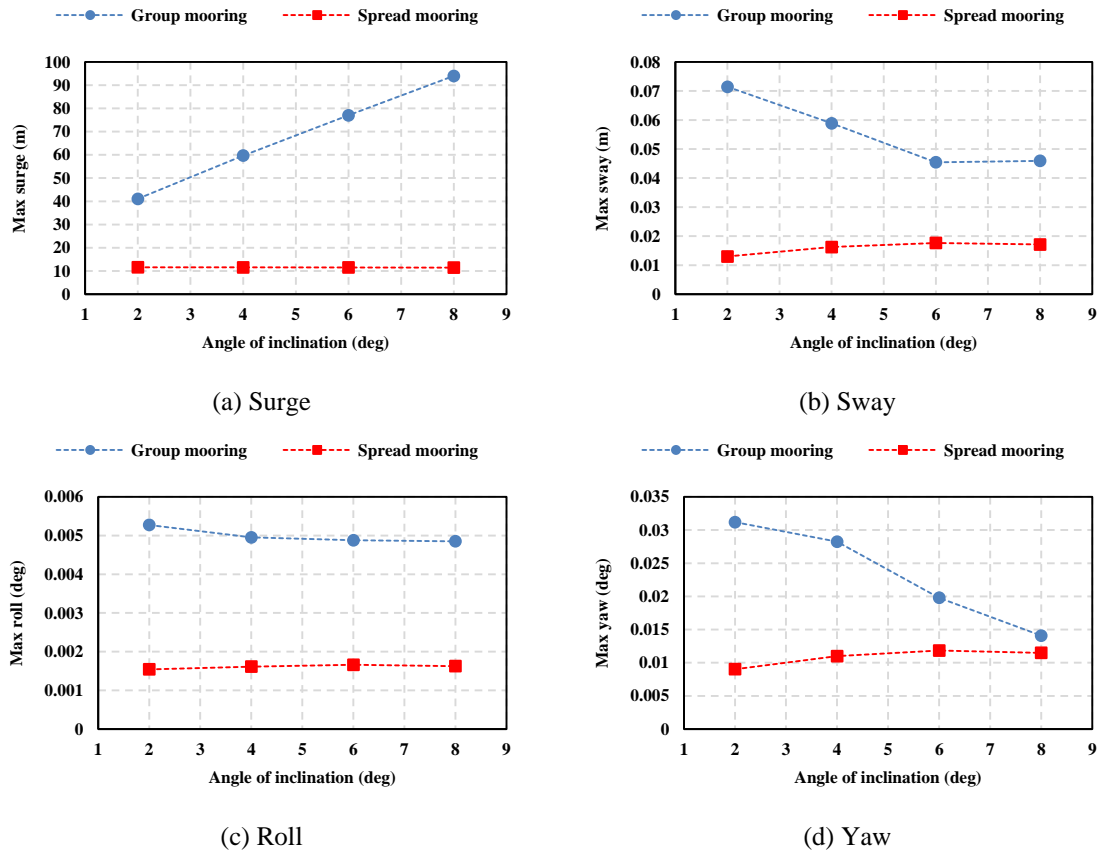


Fig. 11 Effect of different slope bottoms

Fig. 11(a)-11(d) shows the statistical representation of the responses of FPSO in the surge, sway, roll and yaw directions considering group mooring and spread mooring configuration. It is seen that when the angle of inclination increases, maximum surge motions are also monotonously increased, but sway, roll, and yaw motions are gradually decreased for the group mooring. Thus, surge motion is more severe for that mooring configuration in the sloped seabed. Such phenomena might be produced to drift frequency forces. The increased amplitude reaches 25% for group mooring and unchanged for spread mooring in all the seabed angles. In case of sway, roll and yaw motion, the decreased amplitude reaches 10% in group mooring and slightly increased for spread mooring. The motion responses of the Large FPSO are significantly affected by the multi sloped seafloor. Surge, sway, roll, and yaw motions are highly excited in a sloped seabed.

Also, this study proves that spread mooring is more stable than group mooring configuration against structural responses on the sloped seabed.

6. Conclusions

This paper deals with the complex modelling and analysis techniques associated with the nonlinear system of an FPSO as floating rigid body and nonlinear composite mooring lines laid over a sloped seabed. The platform is subjected to combined wave, wind and current loads. Here, the wave is irregular in nature represented by JONSWAP spectrum with high significant wave height. The effect of the seabed has been included in the solution process by introducing an inherent slope in the upstream and downstream side of the FPSO. The ability to model the FPSO as a thin-shelled structure enables panel discretization method and mooring cables as nonlinear catenary multi-segmented lines attached with sloped seabed enable quasi-static analysis method to be implemented by AQWA. Validation of the numerical model has been carried out with an experimental work. To obtain a good estimation of extreme values of slow-drift motions from any numerical simulations a long simulation time is needed. 10000 seconds of longtime simulation to obtain good results in a reasonable time duration with 1.60 GHz processor.

- From the results obtained, the effect of asymmetric stiffness due to the sloped seabed on structural responses is strongly observed. FPSO, surge and sway motions have been increased and roll and yaw motions have been slightly decreased as the difference between stiffness of two mooring sides are gradually increased.
- FPSO Surge motion is more severe as the seabed becomes inclined. However, sway, roll and heave motions are significantly decreased when the sloping bed becomes more inclined.

Taking into account all the computational obstacles while solving a hydrodynamic problem, this extensive comparative investigation reveals the importance of including all system nonlinearities in the governing equations of the rigid body - flexible cable – seabed interaction. The effect of seabed inclination introduces a new modelling scope for the analysis of mooring line behaviour, while simultaneously solving for the responses of floating body in all six DOFs. Further development and research are to be carried out on the system where the effect of seabed inclination is to be investigated by solving the entire problem with cable mass, drag forces, and bending stiffness.

Acknowledgments

This work is supported by National Institute of Technology, Durgapur [grant number NITD/Regis/OR/25].

References

- Baar, J.J.M., Heyl, C.N. and Rodenbusch, G. (2000), "Extreme response of turret moored tankers", *Proceedings of the 32nd Annual Offshore Technology Conference*, Houston, Texas, May.
- Chai, Y.T., Varyani, K.S. and Barltrop, N.D.P. (2002), "Semi-analytical quasi-static formulation for three-dimensional partially grounded mooring system problems", *Ocean Eng.*, **29**, 627-649.
- Faltinsen, O. (1990), *Sea Loads on Ships and Offshore Structures*, Cambridge University Press, Cambridge.
- Irani, M.B., Johnson R.P. and Ward E.G (2001), "FPSO responses to wind, wave and current loading",

- Proceedings of the 20th International Conference on Offshore Mechanics and Arctic Engineering*, Rio de Janeiro, Brazil, January.
- Jones, D.O.B., Mrabure, C.O. and Gates, A.R. (2013), "Changes in deep-water epibenthic megafaunal assemblages in relation to seabed slope on the Nigerian margin", *Deep Sea Research Part I: Oceanographic Research Papers*, **78**, 49-57.
- Kim, S.W., Kim, M.N. and Kang, H.Y. (2016), "Turret location impact on global performance of a thruster-assisted turret-moored FPSO", *Ocean Syst. Eng.*, **6**(3), 265-287.
- Kim, M.H., Koo, B.J., Mercier, R.M. and Ward, E.G. (2005), "Vessel/mooring/riser coupled dynamic analysis of a turret-moored FPSO compared with OTRC experiment", *Ocean Eng.*, **32**, 1780-1802.
- Lee, D.H. (2002), "Nonlinear stability analysis and motion control of tandem moored tankers. Ph.D. Dissertation, Seoul National University, Seoul.
- Lopez, J. T., Taaq, L., Xiao, L. and Hu, Z. (2017), "Experimental study on the hydrodynamic behaviour of an FPSO in a deepwater region of the Gulf of Mexico", *Ocean Eng.*, **129**, 549-566.
- Ormberg, H. and Larsen, K. (1998), "Coupled analysis of floating motion and mooring dynamics for a turret-moored ship", *J. Appl. Ocean Res.*, **20**, 55-67.
- Shivaji, G.T. and Sen, D. (2015), "Direct time domain analysis of floating structures with linear and nonlinear mooring stiffness in a 3D numerical wave tank", *J. Appl. Ocean Res.*, **51**, 153-170.
- Sphaier, S.H., Fernandes, A.C. and Correa, S.H. (2000), "Maneuvering model for the FPSO horizontal plane behaviour", *Proceedings of 10th International Offshore Polar Engineering Conference*, Washington, USA, May-June.
- Tahar, A. and Kim, M.H. (2003), "Hull/mooring/riser coupled dynamic analysis and sensitivity study of a tanker-based FPSO", *J. Appl. Ocean Res.*, **25** (6), 367-382.
- Ward, E.G., Irani, M.B. and Johnson, R.P. (2001), "Responses of a tanker-based FPSO to hurricanes" *Proceedings of the 33rd Offshore Technology Conference*, Houston, Texas, April-May.
- Wichers, J.E.W. (1988), "A simulation model for a single point moored tanker", Ph.D. Dissertation, Delft University of Technology, Delft, Netherlands.